Diffusion tensor imaging metrics in cystic intracranial mass lesions

Amarnath Chellathurai, Priya Muthaiyan, Sathyan Gnanasigamani, Periakarupan Alakappan[1]

Department of Radiodiagnosis, Government Stanley Medical College, [1]Consultant Radiologist, Scansworld Research and Education Institute, Chennai, Tamil Nadu, India

Correspondence: Dr. Priya Muthaiyan, Department of Radiodiagnosis, Government Stanley Medical College, Chennai - 600 001, Affiliated to the Tamil Nadu Dr. M.G.R Medical University, Tamil Nadu, India. E-mail: dr3priya@yahoo.com

Abstract

Background and Purpose: Conventional MR does not always differentiate various cystic lesions of brain. Our purpose was to explore the utility of DTI in characterization & differentiation of intra cranial cystic mass lesions. **Materials and Methods:** DTI was done with a clinical 1.5 Tesla system in 62 patients presenting with intra cranial cystic lesions. Parameter maps of the DTI metrics MD, FA, GA, RA, Geometric tensors (CL,CP,CS) were calculated & quantified using regions of interest. Cystic lesions were grouped based on etiology and management. Statistical analysis was performed to test the significance of difference in DTI metrics in differentiation of various groups of cystic lesions of brain. **Results:** Mann-Whitney U Test was done to analyse the usefulness of various DTI metrics in differentiating the intracranial cysts. Epidermoid cysts showed highest FA, RA, Cl & Cp due to the preferential diffusion of water through the well structured orientation of keratin filaments & flakes within it. Neurocysticercosis showed higher FA, next to epidermoid. Abscesses showed lowest MD. Arachanoid cyst, giant cistern magna, choroid fissure cyst, choroid plexus cyst, ependymal & neuroglial cysts showed higher MD & lower FA, implicating no preferential directional diffusivity. **Conclusion:** DTI does prove useful in characterization and differentiation of intracranial cystic mass lesions. This study implicates the need for inclusion of DTI in the routine protocol of imaging cystic intracranial mass lesions.

Key words: Anisotrophy; cystic intracranial mass lesions; diffusion tensor imaging; diffusion tensor metrics

Introduction

Diffusion-weighted imaging (DWI) deals with restriction of random motion of water molecules which indirectly depicts the nature of the tissue in which these water molecules are moving.[1] It was first described by Brown[2] in 1827 and quantified by Einstein[3] in 1905. Pathological processes which alter the tissue characteristics can therefore be detected by using DWI.[4]

Diffusion tensor imaging (DTI), its derived metrics, tensor shapes, and orientation help us quantify the preferential anisotropic diffusivity of water molecules within a given tissue. It is physically linked to the anisotropy of the tissue structure. This is very well seen in white matter of brain which allows water to diffuse along the course of a fiber rather than perpendicular to it as the axonal membranes and myelin sheaths act as barriers. Every disease process alters directional diffusion in its own unique ways. Fractional anisotropy (FA) and mean diffusion (MD)[5] are two important diffusion tensor parameters, which along with other metrics measure the directional variation, and interactions between these directions provide important information about tissue connectivity.[6]

Access this article online	
Quick Response Code:	Website: www.ijri.org
	DOI: 10.4103/ijri.IJRI_130_17

Cite this article as: Chellathurai A, Muthaiyan P, Gnanasigamani S, Alakappan P. Diffusion tensor imaging metrics in cystic intracranial mass lesions. Indian J Radiol Imaging 2017;27:457-62.

Cysts and cystic appearing intracranial masses are common findings at magnetic resonance imaging (MRI). The spectrum of cystic lesions varies from simple arachnoid cysts to high grade tumors and the management also grossly differs from cysts which require no treatment to those which need radical surgery. This differentiation is sometimes difficult by conventional MRI alone.[7-9] We hypothesize that DTI and the derived indices, FA, MD, geometric tensor metrics, linear anisometry-Cl, planar anisometry-Cp, spherical anisometry-Cs, prove successful in better characterization of these cysts by indirectly reflecting the histological composition of these tissues.

Materials and Methods

The study was started after the approval from the Ethical Committee. Written informed consent was obtained from all the participants. The study group consisted of 62 patients with intracranial cystic lesions – who have come to the Department of Radiology for MRI. Histological diagnosis by surgical resection was obtained in all patients with brain abscess, epidermoid cyst, tumors, and metastases. The diagnosis of benign nonsurgical cyst was confirmed by neuroradiology techniques and infective cysts by posttreatment follow-up. Smaller cysts of size <6 mm were excluded from the study.

Magnetic resonance image acquisition

Imaging was performed on 48-channel SIEMENS AERA system (Germany) 1.5 T using a head coil (40 element), gradient strength of 45 mT, and slew rate of 200 Mt/m/s. The protocol consists of axial, sagittal T1 weighted sequence (T1W), and axial T2 weighted sequence (T2W). DTI was performed in the axial plane by using single-shot echo-planar imaging (EPI) with the following parameters: repetition time (TR)/echo time (TE), 3500/83 ms; diffusion-gradient encoding in 20 directions; b0, 1000 s/mm^2; field of view, 230 × 100 mm; matrix size, 128 × 128; section thickness, 5 mm; bandwidth 1500, EPI factor 128; average 3. Standard DWI acquires data in three orthogonal planes (typically X, Y, and Z axis). By sampling a minimum of six or more diffusion directions with eddy current correction and then establishing a relationship between the acquired data and applied diffusion gradients in the pulse sequence, the directional variation in the tendency of water molecules to diffuse within a voxel was derived. Postprocessing was done using SIEMENS Multimodality Workplace Neuro 3D software.

Data analysis

Diffusion tensor magnetic resonance imaging

Further analysis of the DTI data at the workstation consisted of three major steps[10]: data preprocessing, derivation of tensor metrics, and mapping regions of interest (ROIs). ROI was placed covering more than two-thirds of the cyst area, without touching the lesion wall in all the patients. Distortion–correction for shear, scale, rotation, and translation were done on the obtained raw images, which was then interpolated and decoded to obtain the tensor model for each voxel.[11] Eddy current and subject motion artifact were minimized by co-registering the DWIs on b = 0 images. Finally, tensor diagonalization was done to yield the major (λ1), intermediate (λ2), and minor (λ3) eigenvalues. FA,[5] geometric tensor metrics,[12] Cl, Cp, and Cs, apparent diffusion coefficient (ADC), relative anisometry (RA), geodesic anisometry (GA) were calculated by using standard algorithms. DTI metric values were obtained by placing the ROIs covering more than two-thirds of cystic component.

Statistical analysis

MRI features were assessed by qualified radiologists with more than 10 years of experience. We grouped the cystic lesions into seven groups based on its etiology and management as shown in Table 1. The mean values of DTI metrics for each ROI were compared by using analysis of variance among various groups of cystic lesions. Kruskal–Wallis and Mann–Whitney U test with Bonferroni correction for multiple pairwise comparison were done to compare between the groups, and *P* value <0.05 was considered statistically significant.

Table 1: Grouping of intracranial cystic lesions

Group	Number of cases
GPOUP 1: Maldevelopmental cysts	(25)
Arachnoids cyst	10
Giant cistern magna	2
Choroidal fissure cyst	6
Choroid plexus cyst	2
Ependymal cyst	2
Neuroglial cyst	3
GROUP 2: Acquired porencephalic cyst	(5)
Post op non tumoral cyst	2
Cystic encphealomalacia	2
Radiation necrosis	1
GROUP 3: Neurocysticercosis	7
GROUP 4: Low grade neoplastic cyst	(10)
Ganglioglioma	2
DNET	3
Craniophrangioma	2
Cystic schwannoma	1
Low grade Astrocytoma	2
GROUP 5: High grade neoplastic cyst	(5)
High grade Astrocytoma	2
Astroblastoma	1
Cystic metastasis	2
GROUP 6: Abscess	5
GROUP 7: Epidermoid cyst	5
Total	62

Results

All the cystic lesions were classified into seven groups as described [Table 1]. Our first step was statistical comparison between the groups using Kruskal–Wallis test for each of the DTI metric, which showed a *P* value of <0.001, indicating that the difference in each of the parameter is statistically significant and that our group allocation is perfect. Mann–Whitney U test was then done to analyze the usefulness of various DTI metrics in differentiating the intracranial cysts [Table 2].

Discussion

MD corresponds to ADC or one-third of the trace, which represents the average diffusivity of the media. RA,[5] a normalized standard deviation, is the ratio of the anisotropic part of diffusion to its isotropic part. FA[5] measures the fraction of the "magnitude" of diffusion that can be ascribed to anisotropic diffusion. Generally, FA >0.4 suggests unidirectional structural orientation with high directional diffusivity. FA and RA vary between 0 (isotropic diffusion) and 1 (√2 for RA) (infinite anisotropy). Volumetric ratio (VR) is the ratio of the ellipsoid volume to the volume of a sphere of radius (λ), which range from 1 (isotropic diffusion) to 0. The signal-to-noise ratio of VR is lower than FA and RA. Geometric tensors[13] include linear anisotrophy, planar anisotrophy, and the spherical anisotrophy. In linear anisotrophy, CL, the predominant direction of diffusion is along the direction of the largest eigenvalue (λ̄1> λ̄2 and λ̄3). In planar anisotrophy, CP, the diffusion is restricted to a plane created by two largest eigenvalues (λ̄1, λ̄2> λ̄3). These three coordinates of tensor basics are then normalized to obtain the shape of the tensor, which gives useful information as to the linearity and anisotropy of the concerned structure. GA (Riemann distance) is a geodesic distance on the tensor manifold. It measures the distance of a diffusion tensor to the nearest isotropic tensor, computed intrinsically on the manifold of positive-definite symmetric diffusion tensors. As anisotropy increases, GA changes quite differently from FA. Specifically, GA increases more monotonically than FA. GA may have an advantage over FA for diffusion data with high anisotropy, but it is more susceptible to noise. FA is based on a simple comparison of the tensor eigenvalues. GA, however, measures the deviation of the tensor from the "nearest" isotropic tensor in the associated log-Euclidean metric. GA exploits more of the multivariate information in the diffusion tensor. "b"-value gives the degree of diffusion weighting and is related to the strength and duration of the pulse gradient as well as the interval between these gradients.

Group 1, developmental cysts (n = 25), example arachnoid cysts, show highest MD of 2.838 ± 0.430 × $10^{(-3)}$ mm $^{(2)}$/s and lowest TRACE W = 35 ± 20. These cysts are composed of cerebrospinal fluid (CSF) without much cellular materials, to stop the movement of water molecules which is reflected

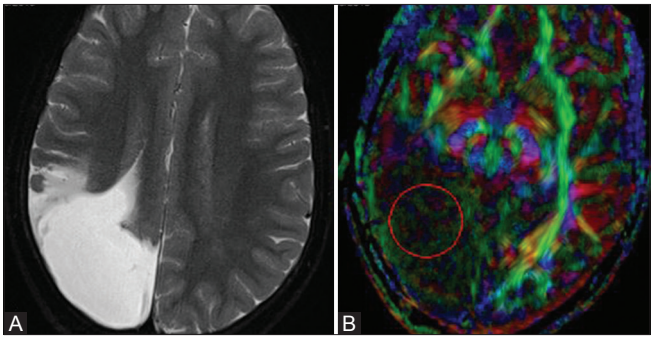

Figure 1 (A and B): (A) T2 weighted MRI. (B) FA map shows a well defined T2 hyperintense porencephalic cyst in the parieto-occipital region

Table 2: Comparison of DTI metrics among various groups

G	MEAN/ MWU	FA	MD	RA	GA	VR	CL	CP	CS	B0	TRACE
1	Mean	0.098±0.03	2.838±0.43	75.05±25.64	138.21±33.06	983.4±23.5	36.68±15.2	55.10±19.9	908.1±32.79	598.2±122.4	35.04±20.04
	MWU	0.931	0.001	0.106	0.001	0.763	0.05	0.042	0.037	<0.001	<0.001
2	Mean	0.05±0.009	2.523±0.90	41.5±4.64	102.8±50.47	996.6±0.85	17.64±3.1	31.0±5.0	951.3±5.83	748.3±168.0	79.06±86.15
	MWU	0.004	0.605	0.001	0.144	0.003	0.010	0.014	0.010	0.359	0.846
3	Mean	0.15±0.19	2.405±0.41	57.37±2.06	95.34±5.03	963.1±21.9	36.78±27.0	63.02±59.8	900.04±86.6	769.7±114.7	50.95±19.46
	MWU	0.002	0.386	0.526	0.164	0.046	0.824	0.920	0.903	0.038	0.541
4	Mean	0.084±0.01	2.691±0.31	64.05±14.5	108.7±28.6	990.09±5.5	28.02±9.57	38.36±13.3	933.7±20.7	672.9±63.0	57.4±21.04
	MWU	0.485	0.612	0.856	0.259	0.667	0.553	0.047	0.221	0.924	0.400
5	Mean	0.06±0.006	2.49±0.65	49.4±5.25	85.6±9.157	995.8±0.89	20.82±2.8	37.6±5.54	941.5±7.55	713.68±93.09	68.04±51.37
	MWU	0.014	0.727	0.05	0.025	0.016	0.074	0.301	0.201	0.493	0.430
6	Mean	0.078±0.01	0.77±0.55	56.84±10.37	78.76±19.12	988.8±10.7	17.64±10.1	37.4±8.84	944.94±18.3	651.0±132.23	239.94±71.8
	MWU	0.289	0.001	0.632	0.009	0.535	0.024	0.196	0.037	0.561	0.003
7	Mean	0.508±0.07	0.86±0.139	477.2±27.38	920.0±42.6	686.2±46.3	218.5±2.08	332.9±5.43	448.62±4.5	859.3±43.7	413.6±27.7
	MWU	<0.001	0.002	<0.001	<0.001	<0.001	<0.001	<0.001	<0.001	0.002	<0.001

(Highlighting the mean of the DTI parameter with statistically significant *P*). Mann-Whitney U-Test significant below *P*<0.05. G: Group, FA: Fractional anisotrophy; MD: Mean diffusivity; RA: Relative anisotrophy; GA: Geodesic anisometry; VR: Volume ratio; CL: Linear tensor; CP: Planar tensor; CS: Spherical tensor

by the highest MD, and very low FA compared to all the other cysts.

Group 2, acquired porencephalic cysts (n = 5) [Figure 1] show lowest FA = 0.056 ± 0.009. These cysts are similar to developmental cysts with lowest FA compared to other cysts.

Group 3, neurocysticercosis (n = 7) [Figure 2] shows second highest mean FA = 0.15 ± 0.19 next to epidermoid, illustrated in the box chart [Figure 3]. The FA values of these cysts show wide variation because it could be in varying stages of evolution. Two of the larger lesions show significantly higher FA values of 0.247 and 0.35, while the smaller cysts of 5–10 mm show lower FA value. Hence, how far it could be generalized for the diagnosis of neurocysticercosis is beyond the limits of our study. The increased FA could be possibly due to the proglottis with four suckers and rostellum of hooklets (which is seen in SPACE sequence) [Figure 2A], cellular sedimentations, and increased viscosity due to the chronicity of these lesions.

Group 4, low-grade tumoral cysts (n = 10) [Figure 2B] show lower mean FA = 0.084 ± 0.013 and MD = 2.69 × $10^{(-3)}$ mm $^{(2)}$/s.

Group 5, high-grade tumoral cysts (n = 5) also show lower mean FA = 0.06 ± 0.007 and MD = 2.49 × $10^{(-3)}$ mm $^{(2)}$/s. Our study was not able to differentiate high from low-grade tumoral cysts. Assis *et al.*, in his study, showed correlation of ADC value in differentiating low-grade and high-grade cysts. Rest of the DTI parameters did not show any significant correlation in their study also.[14]

Group 6, abscess (n = 5) [Figure 4A and B] shows lower mean FA = 0.078 ± 0.018, lowest MD = 0.777 ± 0.55 × $10^{(-3)}$ mm$^{(2)}$/s, and lowest GA = 78.760 ± 19.12 [Figure 4]. The study done by Rakesh K. Gupta *et al.* demonstrates that the abscess cavity has an increased FA compared with other cystic intracranial lesions. This is very much contradictory to the results obtained in our study in that the FA values were less when compared to epidermoid and neurocysticercosis. This could be explained by the fact that epidermoid cysts were not included in their study. One another possibility is that the abscesses could be of varying etiology and stages of evolution. Abscess cavity will have lots of closely packed inflammatory cells, necrotic debris, and proteinaceous materials restricting the extracellular movement of water molecules, which are responsible for lowest MD[12,15-20] obtained in abscess cavity compared to all other cysts.

Group 7, epidermoid cyst (n = 5) [Figure 5A and B] shows highest mean FA = 0.509 ± 0.077, lower

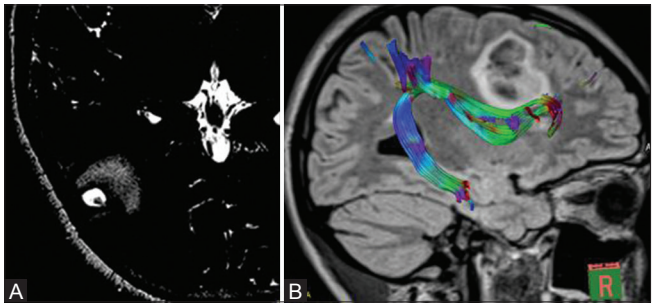

Figure 2 (A and B): (A) SPACE sequence reflecting the gross histopathological structure of scolex with proboscis in a case of neurocysticercosis. (B) Tactography done for a DNET in the right frontal region to map out the eloquent areas preoperatively

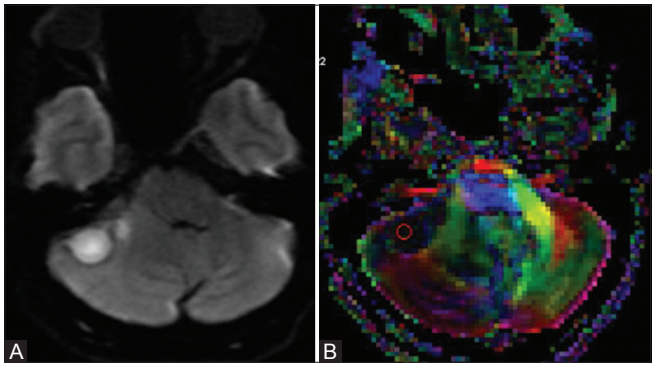

Figure 4 (A and B): (A) DWI showing restriction in a case of abscess in the right cerebellar hemisphere. (B) FA map of the abscess

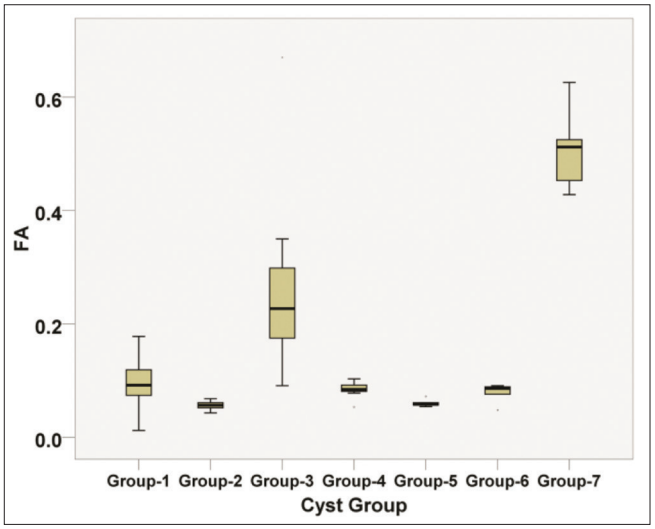

Figure 3: Boxplots of the central regions of FA for groups I–VII

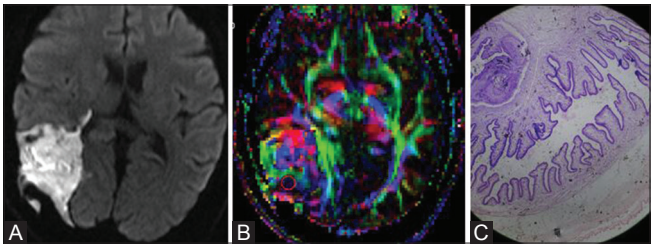

Figure 5 (A-C): (A) DWI showing diffusion restriction in a right parietal lobe epidermoid, (B) FA map of the epidermoid shows multiple lamellated internal structural architecture, (C) Histopathology slide of the above epidermoid

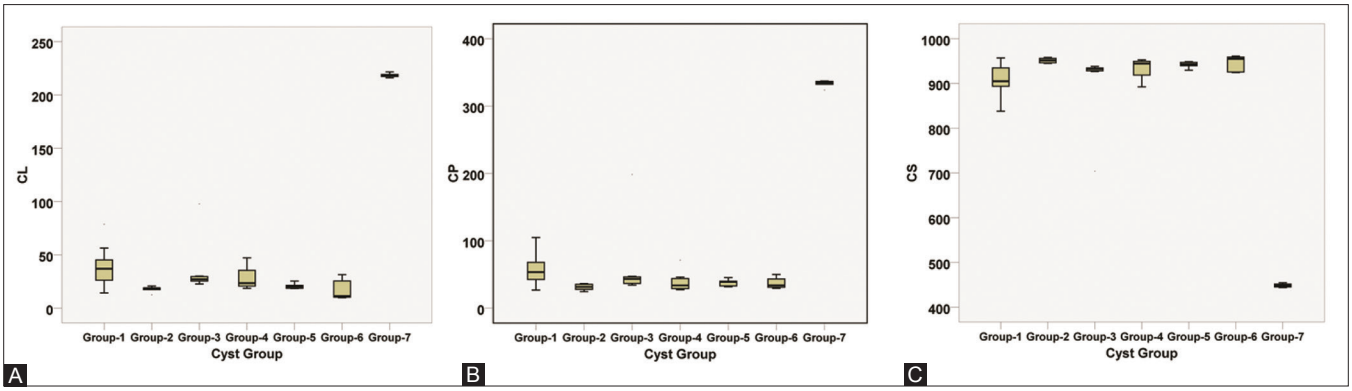

Figure 6 (A-C): Boxplots of the central regions of CL,CP and CS for groups I–VII

MD = 0.866 ± 0.140 × $10^{(-3)}$ $mm^{(2)}$/s, highest RA = 477.200 ± 27.381, lowest VR = 686.200 ± 46.397, highest GA = 920 ± 42.60, grossly different linear component, CL = 218.5, planar component, CP = 332.920, spherical component, CS = 448.62, highest B0 = 859.34 and highest TRACE W = 413.6 ± 27.745 when compared to all other cysts [Figure 6]. Santhosh *et al.*[13] observed a high FA and Cp. Similar results were obtained in our study, indicating a highly structured concentric lamellated internal architecture [Figure 5C] of epidermoid. In addition, our study shows increased Cl and decreased Cs because we have compared epidermoid with rest of the cystic lesions rather than the contralateral white matter as done by Santhosh *et al*. The keratin content of epidermoid cysts was visualized like free water-like in a few number of cases regardless of the sequence used, even though non-CSF material is present within these lesions which could be differentiated only by DTI.

In our study, we were able to differentiate benign cysts [infective, developmental] from malignant cysts.

Limitation of the study

Factors such as cellularity, viscosity, permeability, and histology that can individually affect the diffusivity of water cannot be assessed individually in DTI. All cystic lesions were grouped into seven groups based on the etiology and management, so the differentiations of individual cysts within a group were not possible. In some of the groups the sample size was less. So the significance of each of the parameter could not be generalized. Few other important pathological cysts such as hydatid cyst were not included in our study. Few cysts such as arachnoid cysts were not confirmed by histology.

Conclusion

DTI does prove useful in differentiation of intracranial cystic mass lesions. DTI supports characterization of lesions in addition to routine protocol of imaging in cystic intracranial mass lesions.

Financial support and sponsorship

Nil.

Conflicts of interest

There are no conflicts of interest.

References

1. Pierpaoli C, Jezzard P, Basser PJ, Barnett A, Di Chiro G. Diffusion tensor MR imaging of the human brain. Radiology 1996;201:637-48.
2. Brown R. A brief account of microscopical observations and on the general existence of active molecules in organic and inorganic bodies. The Philosophical Magazine 1828;4:161-73.
3. Einstein A. About the movement of suspended particles in liquids at rest as required by the molecular kinetic theory of heat. Ann Phys 1905;322:549-60.
4. Le Bihan D. Looking into the functional architecture of the brain with diffusion MRI. Nat Rev Neurosci 2003;4:469-80.
5. Dong Q, Welsh RC, Chenevert TL, Carlos RC, Gomez-Hassan DM, Mukherji SK, *et al*. Clinical applications of diffusion tensor imaging. J Magn Reson Imaging 2004;19:6-18.
6. Pajevic S, Pierpaoli C. Color schemes to represent the orientation of anisotropic tissues from diffusion tensor data: Application to white matter fiber tract mapping in the human brain. Magn Reson Med 1999;42:526-40.
7. Mishra AM, Gupta RK, Jaggi RS, Reddy JS, Jha DK, Prasad KN, *et al*. Role of diffusion-weighted imaging and *in vivo* proton magnetic resonance spectroscopy in the differential diagnosis of ring-enhancing intracranial cystic mass lesions. J Comput Assist Tomogr 2004;28:540-7.
8. Reiche W, Schuchardt V, Hagen T, Llyasov KA, Billman P, Weber J. Differential diagnosis of intracranial ring enhancing cystic mass lesions—role of diffusion-weighted imaging (DWI) and diffusion-tensor imaging (DTI). Clin Neurol Neurosurg 2010;112:218-25.
9. Abo-Sheisha DM, Amin MA, Soliman AY. Role of diffusion weighted imaging and proton magnetic resonance spectroscopy in ring enhancing brain lesions. The Egyptian J Radiol Nucl Med 2014;45:825-32.
10. Gupta RK, Hasan KM, Mishra AM, Jha D. High fractional anisotropy in brain abscesses versus other cystic intracranial lesions. AJNR Am J Neuroradiol 2005;26:1107-14.
11. Crank J. The mathematics of diffusion. Oxford: Oxford University Press; 1975. p. 1-10.
12. Toh CH, Wei KC, Ng SH, Wan YL, Lin CP, Castillo M. Differentiation of brain abscesses from necrotic glioblastomas and cystic metastatic brain tumors with diffusion tensor imaging. AJNR Am J Neuroradiol 2011;32:1646-51.
13. Santhosh K, Thomas B, Radhakrishnan VV, Saini J, Kesavadas C, Gupta GK, *et al*. Diffusion tensor and tensor metrics imaging

in intracranial epidermoid cysts. J Magn Reson Imaging 2009;29:967-70.

14. Assis ZA, Saini J, Ranjan M, Gupta AK, Sabharwal P, Naidu PR. Diffusion tensor imaging in evaluation of posterior fossa tumors in children on a 3T MRI scanner. Indian J Radiol Imaging 2015;25:445-52.
15. Desprechins B, Stadnik T, Koerts G, Shabana W, Breucg C, Osteaux M. Use of diffusion weighted MR imaging in differential diagnosis between intracerebral necrotic tumors and cerebral abscesses. AJNR Am J Neuroradiol 1999;20:1252-7.
16. Lai PH, Ho JT, Chen WL, Hsu SS, Wang JS, Yang CF, *et al*. Brain abscess and necrotic brain tumor: Discrimination with proton MR spectroscopy and diffusion-weighted imaging. AJNR Am J Neuroradiol 2002;23:1369-77.
17. Stadnika TW, Chaskis C, Michotte A, Shabana W, Luypaert R, Jellus V, *et al*. Diffusion-weighted MR imaging of intracerebral masses: Comparison with conventional MR imaging and histologic findings. AJNR Am J Neuroradiol 2001;22:969-76.
18. Desprechinsa B, Stadnika T, Koertsa G, Wael S, Breucqa C, Osteauxa M. Use of diffusion-weighted MR imaging in differential diagnosis between intracerebral necrotic tumors and cerebral abscesses. AJNR Am J Neuradiol 1999;20:1252-7.
19. Kunii N. Rathke's cleft cysts: Differentiation from other cystic lesions in the pituitary fossa by use of single-shot fast spin-echo diffusion-weighted MR imaging. Acta Neurochir (Wien) 2007;149:759-69.
20. Reddy JS, Mishra AM, Behari S, Gupta V, Rastogi M, Gupta RK, *et al*. The role of diffusion-weighted imaging in the differential diagnosis of intracranial cystic mass lesions: A report of 147 lesions. Surg Neurol 2006;66:246-50.